

The K/π ratio and the lifespan of the fireball

Boris Tomášik*

*Fakulta prírodných vied, Univerzita Mateja Bela, Tajovského 40,
97401 Banská Bystrica, Slovakia
and Ústav vedy a výskumu, Univerzita Mateja Bela, Cesta na Amfiteáter 1,
97401 Banská Bystrica, Slovakia
E-mail: boris.tomasik@umb.sk*

Evgeni E Kolomeitsev

*University of Minnesota, School of Physics and Astronomy, 116 Church Street SE, Minneapolis,
55455 Minnesota, USA
E-mail: kolomeitsev@physics.umn.edu*

We construct a hadronic kinetic model for description of excitation functions of multiplicity ratios K^+/π^+ , K^-/π^- , and Λ/π . It is shown that the model is able to describe data rather well under the assumption that the total lifespan of the fireball is decreasing function of the collision energy for SPS energies above 30 AGeV. Thus in order to identify the onset of deconfinement the proposed model will have to be checked against other kinds of data until hadronic description can be safely falsified.

*Critical Point and Onset of Deconfinement
July 3-6 2006
Florence, Italy*

*Speaker.

1. Motivation: “the horn”

Very often at this conference possible onset of deconfinement in Pb+Pb collisions at $\sqrt{s_{NN}} \approx 8 \text{ GeV}/c$ has been discussed. Indeed, there are (at least) three interesting excitation functions showing non-monotonic structures just in this collision energy region. Insiders describe them as “the horn”, “the step”, and “the kink” (for review see e.g. [1]). The first relates to the ratio of multiplicities of positively charged kaons and pions. The excitation function of this quantity first rises rapidly to reach a peak around the quoted energy, and then drops down rather sharp and levels off around $\sqrt{s_{NN}} \approx 9 \text{ GeV}/c$ (see e.g. [2]). The second is the mean transverse momentum of kaon spectra which is rising at low energies, is flat roughly in the same region where we observe the horn, and then rises again. Finally, the kink describes the excitation function of the ratio of produced pions per participating nucleon: it starts growing more rapidly just at the same collision energy as the peak of the horn.

Some authors speculate that these observations indicate the onset of deconfined matter. Statistical Model of Early Phase (SMES) [3] reproduces data while it makes a clear assumption that the deconfined phase is reached in the early phase of collision. It is rather schematic, though, and the assumption of almost immediate chemical equilibrium could appear surprising. A kinetic calculation reproducing data on K/π ratio has also been performed [4]. It does not use the argument of early equilibrium. These are positive indications: models which do assume the onset of deconfinement and are capable to accomodate data.

The evidence for transition to plasma of colour charges, however, must be based on exclusion of any hadronic interpretation of data. Several studies went in this direction. Transport generators RQMD and HSD [5] overpredict the π^+ multiplicity. Another BUU model [6] does not show any peak in the K/π ratio. A three-fluid hydrodynamic model [7] with underlying hadronic equation of state reproduces multiplicities of K^+ and pions, but over-predicts the multiplicity of K^- (which is puzzling since the total strangeness must vanish in both theory and experiment). Statistical model assuming full chemical equilibrium [8] shows a maximum of the K^+/π^+ ratio of multiplicities, which is not as high and sharp as the observed one, though. Better agreement with data is obtained if strangeness suppression factor is included in the fit [9]. This opens the question which values of suppression factor are reached during the fireball evolution.

From all these studies a conclusion seems to be emerging that deconfinement must set in at lowest SPS energies, for otherwise data cannot be accommodated. We shall play *advocatus diaboli* here and test a hadronic model on the description of the horn. The horn shall be reproduced successfully, which means that our model will have to be proved on other data also before we can safely exclude it or confirm its validity.

2. Strangeness production in nuclear collisions

Strangeness has been proposed many years ago as a good signal of deconfinement [10]. The simplest argument was that it is energetically cheaper to produce a pair of $s\bar{s}$ quarks in deconfined medium than to produce a pair of $S = \pm 1$ hadrons in hadronic gas. The former requires energy around 300 MeV while most favorable hadronic reaction is $\pi + N \rightarrow K + \Lambda$ with threshold

of 530 MeV above the incoming masses. Thus rates for production of strangeness are naturally expected to be higher in plasma and this should lead to larger total production.

In general, there are two handles to control the final produced amount of strange particles: energy available for strangeness production and time. The former influences the rates. More available energy opens phase space for strangeness-producing reactions and thus increases production rates. The role of time is also rather clear. In a situation of strangeness under-representation the time evolution of the system is always directed towards increasing strangeness content. The longer the system lives, the closer it comes to equilibrium.

The K^+/π^+ ratio is basically a measure of strangeness-to-entropy ratio. Now we wonder if it is possible to combine the available energy and total lifespan of the fireball as functions of collision energy in such a way that we reproduce the horn in strangeness-to-entropy? It is natural to expect that the available energy will be an increasing function of the collision energy. Next, we shall make the assumption that the total lifespan of the fireball shall *decrease* as collision energy increases (Fig. 1). When combining these two features it is imaginable that the strangeness-to-entropy ratio

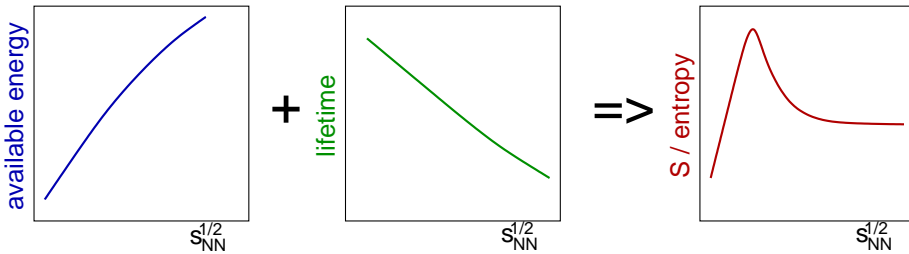


Figure 1: We assume that energy available for production of strange particles increases with collision energy while the lifetime of fireball decreases with increasing collision energy. Then, these two excitation functions might combine into a peak in strangeness-to-entropy ratio as a function of collision energy.

would show a peak. The initial rise is due to increasing available energy which opens larger phase space for production of strange particles. The decrease following the peak is due to shortening time available for strangeness production.

We shall construct a kinetic model for strangeness production and test this hypothesis. In calculating the rates we shall only assume hadronic degrees of freedom.

Before proceeding to the explanation of the model let us comment on the assumption that the lifespan of the fireball decreases with increasing collision energy. There is a widely spread lore that HBT data determine the lifetime to be around 10 fm/c. This is not true! It is important to realize that the measurement of total lifetime via femtoscopy is model-dependent. What is measured is the longitudinal length of homogeneity region. This length can be translated into total lifespan only with help of a model (Fig. 2). Usually, Bjorken model [11] is used and this is where the quoted 10 fm/c comes from. If, however, there is nuclear stopping and the expansion of the fireball is to a large extent built up from pressure, then Bjorken scenario is invalid and the measured longitudinal size may be reached after a longer lifespan. An implication of this is that longer lifespan does not necessarily mean larger freeze-out volume and larger multiplicity. Various physics can lead to prolonged lifetime. Stopping and reexpansion is one possibility. Another possibility is softening of the equation of state, i.e., weak pressure gradients which do not enough accelerate expansion.

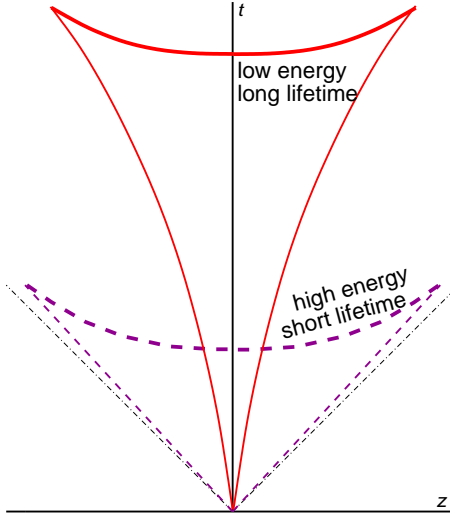


Figure 2: Longer lifetime of a fireball does not necessarily imply larger extent in longitudinal direction. Evolution scenarios and freeze-out hypersurfaces in a space-time diagram for fireballs created at lower collision energy with strong stopping and re-expansion (solid line), and higher collision energy in nuclear transparency regime (dashed line).

3. A kinetic model of strangeness production

We shall perform numerical kinetic calculation of strangeness production. In its spirit, the model is very similar to early works on strangeness production [12, 13, 14] and later flavour-kinetic [15, 16] or hydro-kinetic [17] simulations. In contrast to the later, we do *not* calculate the space-time evolution in framework of a hydrodynamic model. We *parametrise* it. The reason for this approach is that we know from femtoscopic studies that hydrodynamic simulations do not reproduce sizes of the fireball at breakup. Therefore, there is no reason to pretend that they give the correct space-time evolution of the fireball. On the other hand, if we *parametrise* the evolution, we have the freedom to explore various different fireball evolution scenarios and identify those which best correspond to data. We shall go this way.

Since we shall only calculate the ratios of multiplicities and not the multiplicities themselves we do not need to calculate the volume of the system; it shall suffice to know the *average* densities of species. In particular, we shall calculate and evolve densities of kaons with $S = 1$. These follow the master equation

$$\frac{d\rho_K}{d\tau} = \frac{d}{d\tau} \frac{N_K}{V} = -\frac{N_K}{V} \frac{1}{V} \frac{dV}{d\tau} + \frac{1}{V} \frac{dN_K}{d\tau}. \quad (3.1)$$

Obviously, the first term on the right hand side includes the expansion rate $1/V dV/d\tau$ and stands for the change of density solely due to expansion. The second term represents the change of density resulting from kaon production and/or annihilation. It can be split into two terms: production rate and annihilation rate. Thus the resulting master equation generally reads

$$\frac{d\rho_K}{d\tau} = \rho_K \left(-\frac{1}{V} \frac{dV}{d\tau} \right) + \mathcal{R}_{\text{gain}} - \mathcal{R}_{\text{loss}}. \quad (3.2)$$

In hydro-kinetic or flavour-kinetic approaches, the expansion rate follows from hydrodynamic calculation. We shall use an *ansatz* for the evolution of energy and baryon densities. The ansatz concerning baryon density evolution will enter into our calculation through the expansion rate.

3.1 Production and annihilation

From Eq. (3.2) we calculate densities of K^+ , K^0 , K^{*+} , and K^{*0} . Throughout our calculation we assume that all particles keep their vacuum properties.

The gain term in Eq. (3.2) includes two types of contributions

$$\mathcal{R}_{\text{gain}} = \sum_{ijX} \langle v_{ij} \sigma_{ij}^{KX} \rangle \frac{\rho_i \rho_j}{1 + \delta_{ij}} + \rho_{K^*} \Gamma_{K^*}, \quad (3.3)$$

where the sum goes over two-to-N processes leading to production of kaons and the second term is for K^* decay into K . In angular brackets we have the cross-section multiplied with relative velocity of the relative pair and averaged over all relative velocities. In this averaging we assume thermal distribution of velocities. Thus kaons are assumed to be in *thermal* equilibrium until the decoupling. The loss term includes processes which destroy kaons and is obtained in a similar way

$$\mathcal{R}_{\text{loss}} = \sum_{iX} \langle v_{Ki} \sigma_{Ki}^X \rangle \frac{\rho_K \rho_i}{1 + \delta_{Ki}}. \quad (3.4)$$

In practice, it is impossible to include *all* reactions which create or destroy a kaon. Most of them, particularly those involving heavier particles, have unknown and/or poorly constrained cross-sections. Their influence, however, is not so important. Due to large mass the abundance of heavy particles is small and the rate of corresponding processes is low. We implement following reactions in our calculation:

- Associated production of kaon and hyperon in reactions of pions with N and/or Δ . Kaon annihilation on hyperons leading to N or Δ with pion is also taken into account.
- Meson reactions of $\pi\pi$, $\pi\rho$, and $\rho\rho$ leading to $K\bar{K}$ production are included in both directions: creating and destroying kaons.
- Production of K^* from K and π and its decay.
- Reactions of $\pi Y \leftrightarrow K\Xi$, these are also included in both directions.
- Baryon-baryon reactions of NN , $N\Delta$, and $\Delta\Delta$ which produce kaons lead to more than two particles in the final state and are included only in kaon gain term.

Species other than kaons with $S = 1$ are treated according to equilibrium assumptions. The non-strange species are assumed to be in chemical equilibrium. This follows from the assumption that inelastic processes among them are quick and able to keep the chemical equilibrium. Species with $S < 0$ (i.e. those containing strange quark) must balance the abundance of strange antiquarks contained in kaons. We assume, that strong interactions which do not create but just reshuffle strange quarks between two particles are fast enough to keep the $S < 0$ particles in *relative* chemical equilibrium.

In principle, *all* reactions can be treated kinetically. However, it appears that the assumptions of equilibria bring the model closer to how real process actually runs. There are many reactions with poorly known or unknown cross-sections. Unlike in strangeness production, here these processes may have important influence on the relaxation time. Due to the large variety of possible processes and presumably large cross-sections the relevant relaxation times shall be small enough in order to keep the non-strange sector of the whole system in equilibrium. Incomplete calculation with wrong cross-sections, on the other hand, may deviate from this strongly. Since a complete kinetic calculation is technically not possible, it is safer to *assume* (partial) chemical equilibrium and calculate abundances from this assumption.

Finally, let us note that we included no antibaryons into our calculations. Since the system represents baryon-rich environment, we do not expect a big error connected with this simplification. The amount of antibaryons grows with collision energy. At the highest SPS energy the ratio of $\bar{\Lambda}/\Lambda$ multiplicities is around 10%, so this gives us an upper estimate for the error we commit here.

3.2 The ansatz for expansion

It will be assumed that the evolution of fireball densities consists basically of two periods. First, the expansion is accelerated due to internal pressure of the matter. Here we shall assume the simplest parametrisation of accelerating expansion: quadratic dependence on time. Afterwards, the expansion turns into a scaling scenario with power law decrease of baryon density, as it is commonly assumed and in accord with femtoscopy measurements. Since baryon number is conserved quantum charge, the time dependence of average baryon density gives the evolution of inverse volume. We assume that is goes like

$$\rho_Q(\tau) = \begin{cases} \rho_{Q0}(1 - a\tau - b\tau^2)^\delta & : \tau < \tau_s \\ \frac{\rho'_{Q0}}{(\tau - \tau_0)^\alpha} & : \tau \geq \tau_s \end{cases} \quad (3.5)$$

where ρ_{Q0} , a , b , ρ'_{Q0} , τ_0 , τ_s , α and δ are parameters which can be tuned. They can be more conveniently expressed in terms of total lifespan, initial baryon density, initial expansion rate, maximum expansion rate, etc. [18]. We shall change these parameters and thus explore a wide range of possible evolution scenarios. Our models may vary “in between” the commonly known Bjorken [11] and Landau [19] models.

The energy density is parametrised similarly to baryon density. The equation of state enters in a simple way by relating the equation for energy density to that for baryon density through the exponent δ

$$\varepsilon(\tau) = \begin{cases} \varepsilon_0(1 - a\tau - b\tau^2) & : \tau < \tau_s \\ \frac{\varepsilon'_0}{(\tau - \tau_0)^{\alpha/\delta}} & : \tau \geq \tau_s \end{cases} \quad (3.6)$$

3.3 Initial and final conditions

We already specified the master equation and its ingredients. It remains to determine the initial conditions. Clearly, strange particles are first produced in primordial collisions of incoming nucleons. The corresponding “initial” densities of K^+ and K^0 are estimated from data on proton-proton collisions and extrapolations to nucleon-nucleon collisions [20]. The initial densities of

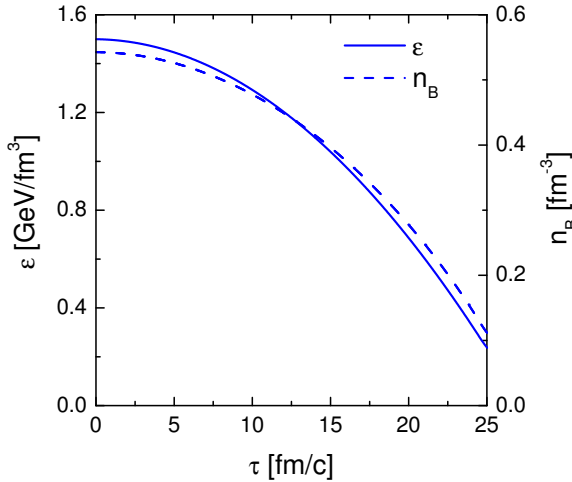


Figure 3: Time evolution of energy density (solid line, left scale) and baryon density (dashed line, right scale) in a model which reproduces the data from Pb+Pb collisions at projectile energy 30 AGeV.

species with $S < 0$ are then obtained by making use of the requirement that total strangeness must vanish. Ratios of these densities are fixed according to the assumption of relative equilibrium.

In order to choose a specific model, we must fix parameters which appear in Eq. (3.5). The most important quantities which are selected are the initial energy density ε_0 and the total lifespan τ_T . Furthermore, our simulation must arrive to the final state which corresponds to chemical freeze-out. Thus we fix the final values of energy density, baryon density, and the density of third component of isospin. These we infer from chemical freeze-out fits of [9].

In this way, we are guaranteed by construction to arrive at the correct final state energy and baryon density. Notice, however, that this does not automatically warrant the correct temperature. At fixed energy density the temperature depends on the effective number of degrees of freedom and thus the resulting temperature will depend on the amount of produced strange particles, which is calculated kinetically.

The argument can be pushed further. *If* the density of strange particles comes out correct, then the temperature and baryochemical potential are also correct. In such a case, abundances of *all* species are correct, since they are calculated statistically.

3.4 Examples: time evolution of densities

Before presenting the results, let us illustrate the time evolution of densities. We see in Fig. 3 that most of the time the fireball stays in the accelerating phase characterised by the quadratic dependence of density on time. This feature is rather general in our model. It is so because of the requirement of rather low initial energy density. If the power-law time dependence of the second phase was realised for a longer time, this would require very high initial energy density reaching up to tens of GeV/fm^3 .

In Fig. 4 we show the evolution of the density of K^+ . If only the density is plotted, we observe rise followed by rapid decrease; the former is due to quick kaon production in a slowly expanding fireball with strongly under-represented strange particles, while the latter is mainly due to strong expansion and corresponding decrease of all densities. In order to extract the net effect

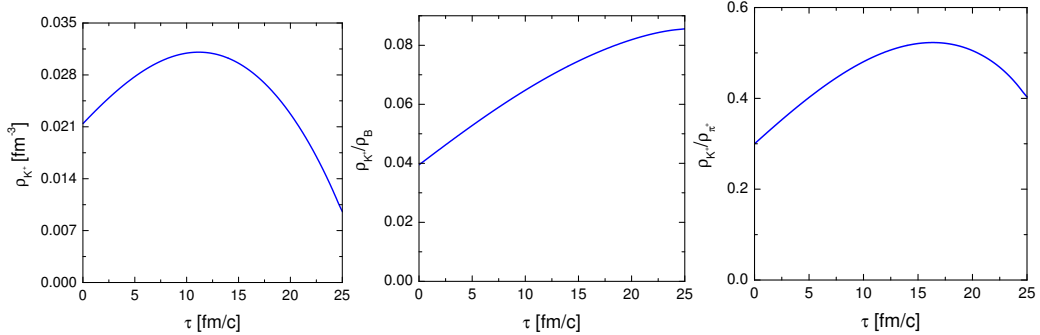


Figure 4: The evolution of K^+ density (left), K^+ density divided by baryon density as a density of conserved quantum charge (middle), and K^+ density divided by π^+ density.

of kaon production one can divide K^+ density by baryon density which drops with time only due to expansion. The ratio ρ_K/ρ_B increases steadily, though the growth becomes slower at later times when kaon abundance becomes larger.

Finally, we also show in Fig. 4 the time-dependence of the ratio of densities of positive kaons and pions. The final value is about a factor of 2 larger than data value of 0.23, so it may seem confusing if we say that this scenario reproduces data. The point is that in the value which is compared with data we also take into account feed-down from resonance decays, which is not yet included in Fig. 4. The feed-down contributes more to pion density in the denominator and brings the final value close to measured data.

We want to close this section with a brief explanation of how the final density of various strange species can be controlled. We shall calculate ratios of multiplicities K^+/π^+ , K^-/π^- , and Λ/π . Density of kaons with $S > 0$ is produced kinetically and depends dominantly on the total lifespan and slightly on temperature. Thus the lifespan is decisive for ratio of K^+/π^+ . Species with $S < 0$ must balance strangeness such that total S of the system vanishes. Strange quarks are distributed among K^- and hyperons according to equilibrium distribution. Hence, once we have the correct amount of K^+ , the final state temperature determines if we obtain correct results also for K^- and Λ 's.

4. Results and discussion

Typical results are presented in Figs. 5 (Pb+Pb at projectile energy 30 AGeV), 6 (158 AGeV), and 7 (Au+Au at 11.6 AGeV). We observe that the ratios of strange particles to pions depend strongly on the total lifespan of the fireball. One should not get confused. What is plotted is dependence of the *final state ratio* on *total lifespan*; it is *not* the evolution of the ratios with time. In other words, every plotted point in the figures corresponds to a different parametrisation of fireball evolution.

Compared to the dependence on total lifespan, the dependence on initial energy density appears less pronounced. It is more important in collisions at lower energies which produce matter at higher net baryon densities.

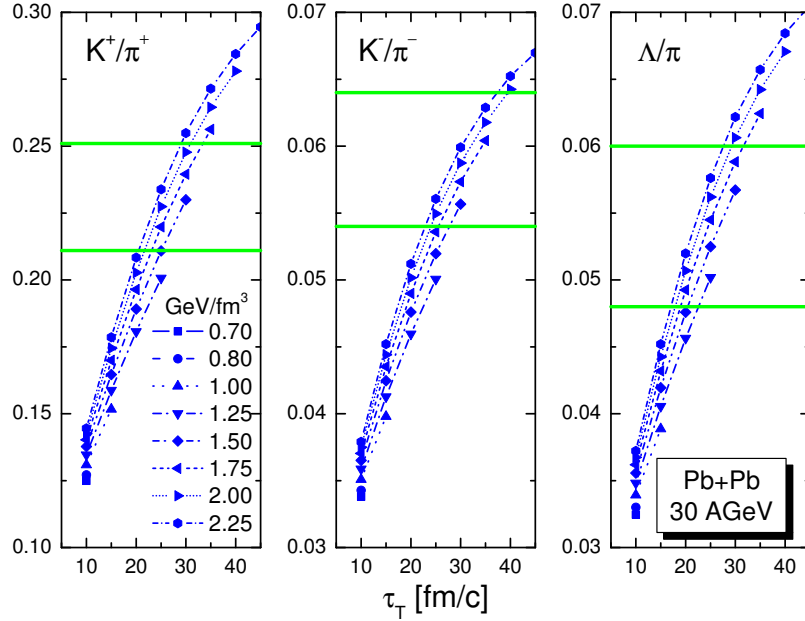


Figure 5: Dependence of the resulting ratios of K^+/π^+ multiplicities (left), K^-/π^- (middle), and Λ/π (right) on total lifespan of the fireball calculated for Pb+Pb collisions at projectile energy 30 AGeV. Different curves correspond to different initial energy densities according to legend.

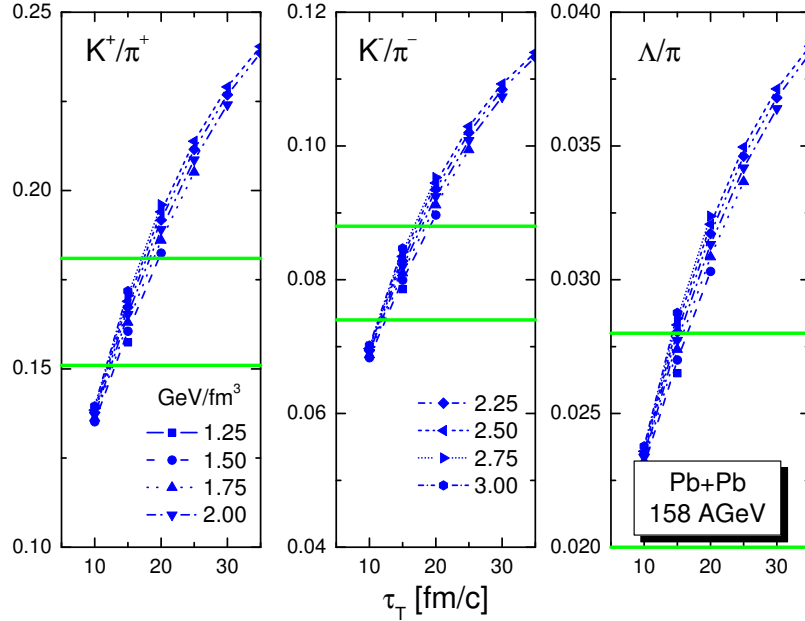


Figure 6: Same as Fig. 5, but for Pb+Pb collisions at projectile energy 158 AGeV.

In order to reasonably compare our results with data, for every triple of calculated ratios we construct a quantity χ^2 which is determined as

$$\chi^2 = \sum_{i=1}^3 \frac{(d_i - t_i)^2}{e_i^2} \quad (4.1)$$

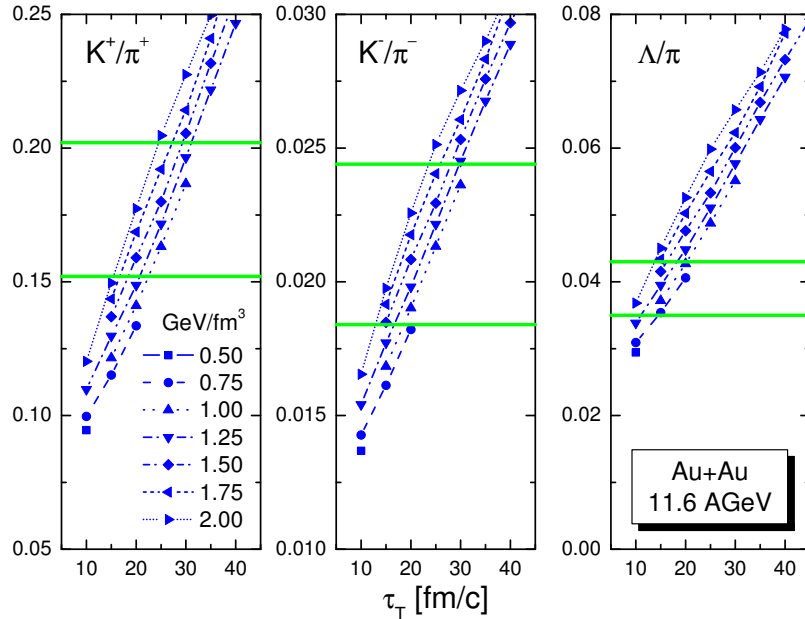


Figure 7: Same as Fig. 5 but for Au+Au collisions at projectile energy 11.6 AGeV.

where t_i , d_i , and e_i stand for theoretical value, data value, and its error, respectively. The sum goes over the three density ratios calculated here. The values of χ^2 calculated according to this prescription are summarised in Fig. 8. With this figure we want to test the hypothesis put forward in Fig. 1: can a combination of increasing available energy and *decreasing* total lifespan explain the observed horn? From Fig. 8 we see that the horny structure of K^+/π^+ ratio is basically translated into a similar dependence of the “best” total lifespan on collision energy. One could speculate if this is really the case that the fireball lives longest at lowest SPS energy. This could be reminiscent of an evolution in the soft region of the equation of state. Still, instead of making such a conclusion we want to note that the quality of data does not allow to draw this kind of conclusions very clearly. In fact, one can still reproduce data with rather acceptable quality by scenarios whose lifespans do not increase with the collision energy. We summarise our choice of such scenarios in Table 1.

Finally, in Fig. 9 we show the comparison of data to results obtained with scenarios displayed in Table 1. The data are reproduced rather well. Note that we did not perform any calculations

E_{beam} [AGeV]	11.6	30	40	80	158
ϵ_0 [GeV/fm 3]	1	1.5	2	2.25	2.75
τ_T [fm/c]	25	25	20	15	15
T [MeV]	118.1	139.0	147.6	153.7	157.8
T_f [MeV]	114.7	134.1	143.3	149.3	153.6

Table 1: Initial energy densities and total lifetimes from parameter sets which were used in calculations leading to results shown in Fig. 9. In the lower portion of the table T_f is the final state temperature obtained in our simulations and T the temperature from the analysis of chemical freeze-out [9].

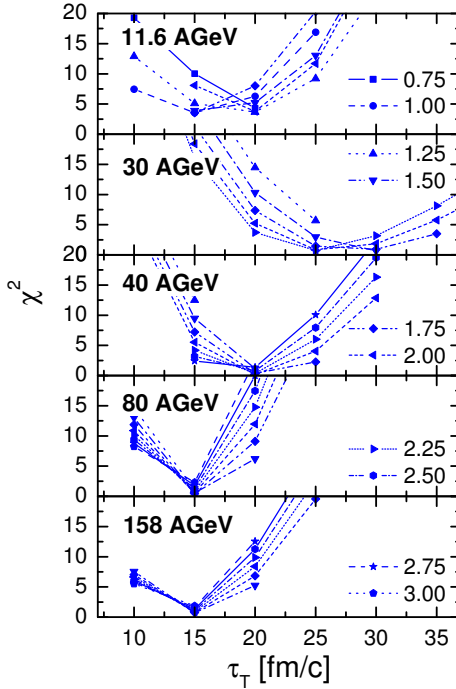


Figure 8: Values of χ^2 determined from Eq. (4.1). Different panels correspond to collisions at different energy. χ^2 is shown as a function of total lifespan; different curves represent different initial energy densities.

for the data point at projectile energy of 20 AGeV (data points at second lowest energies) as no tabulated data were available to us. The slight failure of our model at lowest collision energies is due to disagreement in the Λ/π ratio.

5. Conclusions

We managed—with a solely hadronic kinetic model—to reproduce the famous “horn”: excitation functions of multiplicity ratios of K^+/π^+ , K^-/π^- , and Λ/π . Therefore, merely these data do not suffice for rejection of hadronic model of fireball evolution and do not allow for convincing claims that deconfinement sets in at collision energy where the horn appears. In our framework, description of data requires decreasing total lifetime as a function of collision energy at least for beam energies above the horn.

Hence, in order to reject hadronic description comparisons with other types of data must be undergone. The model—if applicable—must be able to describe also single-particle spectra, correlations, as well as total abundances. Dilepton spectra appear as particularly interesting since dileptons are emitted throughout the whole evolution of the fireball and thus are sensitive to the total lifespan.

Finally, so far we put off the question, what microscopic mechanism or equation of state leads to a total lifespan decreasing with increasing collision energy. If our hadronic kinetic model in which time evolution is only parametrised survives all data tests, the quest for underlying microscopic mechanism must be taken up.

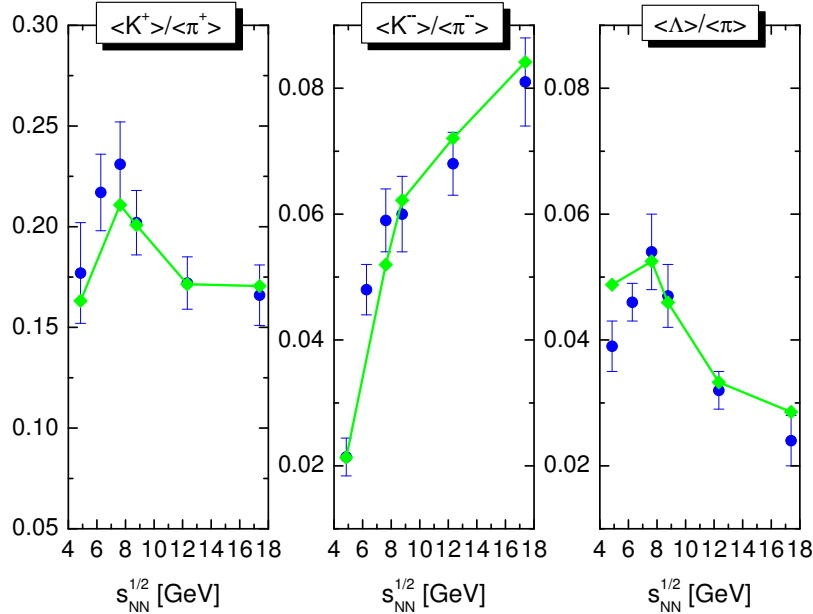


Figure 9: Comparison of data with selected results of our simulations. Plotted are excitation functions of multiplicity ratios of K^+/π^+ (left panel), K^-/π^- (middle), and Λ/π (right). Data points are from [2].

Acknowledgments

BT thanks the organisers for invitation and kind hospitality in Florence. He also thankfully acknowledges OZ Príroda for partial support of the trip. The work presented here has been supported by a Marie Curie Intra-European fellowship within the 6th European Community Framework programme (BT) and by the US Department of Energy under contract No. DE-FG02-87ER40328 (EEK).

References

- [1] G. Roland, these proceedings.
- [2] B. Lungwitz for the NA49 collaboration, AIP Conf. Proc. **828** (2006) 321.
- [3] M. Gaździcki, M.I. Gorenstein, Acta Phys. Pol. B. **30** (1999) 2705
- [4] J.K. Nayak, J.e. Alam, P. Roy, A.K. Dutt-Mazumder, B. Mohanty, Acta Phys. Slov. **56** (2005) 27.
- [5] E.L. Bratkovskaya *et al.*, Phys. Rev. C **69** (2004) 054907.
- [6] M. Wagner, A.B. Larionov, U. Mosel, Phys. Rev. C **71** (2005) 034910.
- [7] Yu.B. Ivanov, V.N. Russkikh, V.D. Toneev, Phys. Rev. C **73** (2006) 044904.
- [8] J. Cleymans, H. Oeschler, K. Redlich, S. Wheaton, Phys. Lett. B **615** (2005) 50.
- [9] F. Becattini, M. Gaździcki, A. Keränen, J. Manninen, R. Stock, Phys. Rev. C **69** (2004) 024905.
- [10] J. Rafelski, Phys. Rep. **88** (1982) 331.
- [11] J.D. Bjorken, Phys. Rev. D **27** (1983) 140.

- [12] P. Koch and J. Rafelski, Nucl. Phys. A **444** (1985) 678.
- [13] P. Koch, B. Müller, J. Rafelski, Phys. Rep. **142** (1986) 167.
- [14] J.I. Kapusta and A. Mekjian, Phys. Rev. D **33** (1986) 1304.
- [15] H.W. Barz, B.L. Friman, J. Knoll, H. Schulz, Nucl. Phys. A **484** (1988) 661.
- [16] H.W. Barz, B.L. Friman, J. Knoll, H. Schulz, Nucl. Phys. A **519** (1990) 831.
- [17] G.E. Brown, C.M. Ko, Z.G. Wu, L.H. Xia, Phys. Rev. C **43** (1991) 1881.
- [18] B. Tomášik and E.E. Kolomeitsev, nucl-th/0512088.
- [19] L.D. Landau, Izv. Akad. Nauk SSSR, Ser. Fiz., **17** (1953) 51.
- [20] M. Gaździcki and D. Röhrich, Z. Phys. C **71** (1996) 55.